

SmartCar: Detecting Driver Stress

Jennifer Healey and Rosalind Picard

Massachusetts Institute of Technology

Media Laboratory

20 Ames St, Cambridge MA, USA

fenn, picard@media.mit.edu

Abstract

Smart physiological sensors embedded in an automobile afford a novel opportunity to capture naturally occurring episodes of driver stress. In a series of ten ninety minute drives on public roads and highways, electrocardiogram, electromyogram, respiration and skin conductance sensors were used to measure autonomic nervous system activation. The signals were digitized in real time and stored on the SmartCar's pentium class computer. Each drive followed a pre-specified route through fifteen different events, from which four stress level categories were created according to the results of the subjects self report questionnaires. In total, 545 one minute segments were classified. A linear discriminant function was used to rank each feature individually based on recognition performance and a sequential forward floating selection (SFFS) algorithm was used to find an optimal set of features for recognizing patterns of driver stress (88.6%). Using multiple features improved performance significantly over the best single feature performance (62.2%).



1 Introduction

Stress has been identified as an important health risk, contributing adversely to chronic problems such as back pain and migraine headaches and to life threatening conditions such as cardiac arrest and cancer, yet the problem of accurately detecting, recording and quantifying the salient features of stress remains a challenge to health professionals and researchers. Many features of physiological signals have been proposed as indicators of stress by cardiologists and psychophysicists, but these are usually evaluated individually and their performance for recognition is seldom tested. This paper shows how pattern recognition techniques can be applied to identify the best combinations of features to detect stress in automobile drivers derived from four physiological sensor signals: electromyogram (EMG - \mathcal{E}), electrocardiogram (EKG), galvanic skin response (GSR - \mathcal{G}) and respiration through chest cavity expansion (\mathcal{R}). These signals were chosen because previous studies have found them useful for assessing arousal and stress[ELF83]. GSR has been noted as being particularly useful in studying driver stress[Hel78]. For this analysis, a SmartCar system was developed to collect physiological data from natural driving situations along with multiple



Figure 1: Above: a sample frame from the video collected during the experiment showing driver facial expression and road conditions synchronized to the real-time physiological responses. Below: a diagram showing sensor placement. GSR sensors are placed on both the hand and the foot.

Event Num.	Event Description	Stress Rating
1.	Beginning stationary period (rest1)	1
2.	Garage Exit	2
3.	City Road (city1)	4
4.	Toll Booth (toll1)	3
5.	Highway driving period (hwy1)	3
6.	Toll Booth (toll2)	3
7.	Exit Ramp Turnaround (exit)	5
8.	Toll Booth (toll3)	3
9.	Highway driving period (hwy2)	3
10.	Two Lane Merge (merge)	5
11.	Toll Booth (toll4)	3
12.	Bridge crossing (bridge)	4
13.	City Road (city2)	4
14.	Enter Garage	1
15.	End stationary period (rest2)	1

Table 1: A summary of driving events and the median stress rating from the ten questionnaires

video recordings to provide ground truth for validation. Four stress categories were defined by a questionnaire analysis of perceived stress ratings. Twelve features characterized each of 545 one minute data segments taken from the ten days of driving records. Each of these segments was labeled as belonging to one of four stress categories: low, neutral, high or very high stress.

2 Data Collection

A SmartCar system was developed for this experiment by augmenting a car with an on-board Pentium computer with video cameras a microphone and four physiological sensors. Figure 1 shows the placement of the sensors on the subject and the composite image record of the video cameras plus the video feed from the computer monitoring the sensors. The driving route was designed to simulate a commute to work. Table 1 shows a sequential list of the driving events as they were encountered and the median stress rating given to that event by the median of the questionnaires scores which ranged from "1" to "7." From these ratings four stress categories were created: very high (events 7,10), high (events 3, 12, 13), neutral (events 4,5,6,8,9) and low stress (events 1,2 14,15). The toll events and the garage exit were excluded from analysis due to excessive motion artifacts and inconsistencies in the experimental protocol.

3 Feature Extraction

Ten complete records of physiological data were collected from this experiment. Each record consists of approximately ninety minutes of data, however, the length of time for the experiment and for each of the fifteen driving driving events varied from day to day due to traffic conditions. From the records 545 one minute segments were extracted which belonged to one of the fifteen driving categories in Table 1.

From each of the one minute segments the following features were extracted: the mean and variance of the signals \mathcal{E} , \mathcal{G} , and \mathcal{R} , represented respectively by the symbols: $\mu_{\mathcal{E}}$,

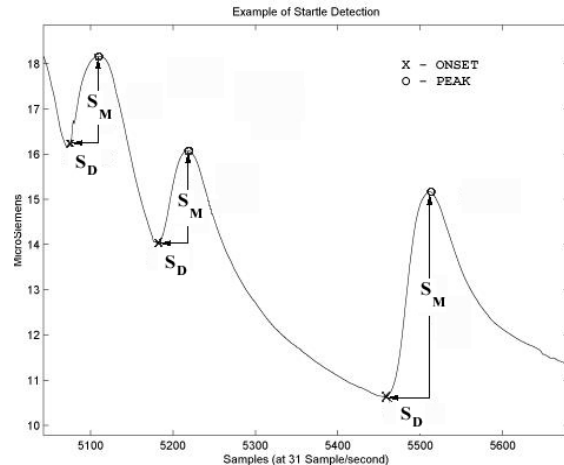


Figure 2: An example of GSR responses occurring in a one minute segment and the results of the algorithm showing onset "X" and peak "O" detection. The features S_M and S_D are derived as shown.

$\sigma_{\mathcal{E}}$; $\mu_{\mathcal{G}}$, $\sigma_{\mathcal{G}}$; and $\mu_{\mathcal{R}}$, $\sigma_{\mathcal{R}}$; features of the GSR orienting response, including the frequency of occurrence S_F , the sum of durations ΣS_D , the sum of magnitudes ΣS_M and the sum of the estimated areas ΣS_A . Two features were derived from the EKG signal, the heart rate (HR) and autonomic balance (AB) from short term power spectrum heart rate variability.

Four features of the GSR response are derived from an algorithm which detects the onset and peak of individual responses, as shown in Figure 2. The detection algorithm first smoothes the segment using a digital elliptical filter with a cutoff at 4Hz. Next the derivative of the signal was calculated using the first forward difference ($\delta_{\mathcal{G}}[n] = \mathcal{G}[n] - \mathcal{G}[n-1]$) and a threshold was applied ($0.093 \mu S$ per sec was found to yield good performance in practise). Responses occurring less than one second after a previous response were counted as a continuation of that response. Once the response was detected, the zero-crossings of the derivative preceding and following the response were identified as the onset and peak of the response respectively. The features for the magnitude S_M and duration S_D of each response are derived as:

$$S_M = t_{peak} - t_{onset} \quad (1)$$

$$S_D = \mathcal{G}_{peak} - \mathcal{G}_{onset} \quad (2)$$

From these measurements the area of the response is estimated by $S_A = \frac{1}{2} * S_M * S_D$. For each one minute segment, the sum of response magnitudes (ΣS_M), durations (ΣS_D), areas (ΣS_A) and the frequency of responses (S_F) are calculated.

The AB feature is calculated by finding the ratio of low frequency energy to high frequency energy in the spectrum of the heart rate (HR) signal. This feature used a five minute window of the heart rate time series centered on the midpoint of the minute segment used for the other features. To calculate AB, the heart rate time series was first derived from the EKG signal by detecting the

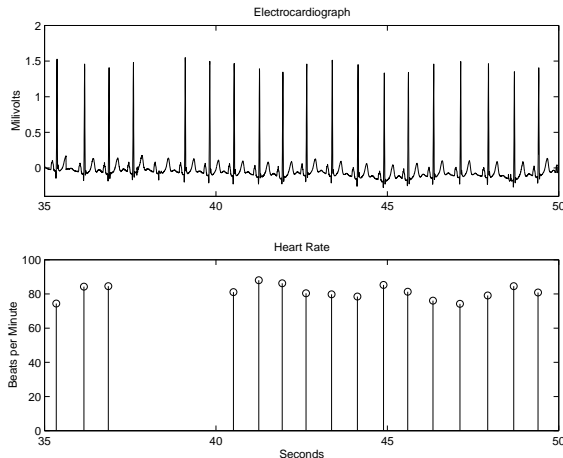


Figure 3: Above: The peaks or the “R” waves in the electrocardiograph signal are first detected using the WAVE software[Moo93]. Outliers in the heart rate time series, caused by missed beats are ignored rather than estimated. A Lomb-Scargill periodogram is then calculated on this time series.

amount of time between successive “R” wave peaks in the EKG. These peaks were detected using the WAVE software program developed by George Moody (available at <http://ecg.mit.edu>). This program was used to reject outliers as shown in Figure 3 and use a least-squares spectrum estimation (Lomb-Scargill) method to determine heart rate variability[Moo93] [Lom76]. Autonomic balance is a measure of the variability of the time series of the heart rate derived from the EKG. The low frequency (LF) variations in the heart rate (0.01-0.08 Hz) are influenced by both sympathetic and parasympathetic activity, while the high frequency (HF) variations (0.15-0.5 Hz) are almost exclusively due to parasympathetic activity[SSea93]. The ratio of low to high frequency energy and reflects the sympathovagal balance, a measure that increases in stressful situations and decrease with relaxation[MAea95]. The ratio of the sum of the energy in the LF band of this spectrum to the HF band is then calculated as the AB feature:

$$AB = \frac{LF}{HF} = \frac{\sum_{0.01}^{0.08} lombPSD(HR)}{\sum_{0.15}^{0.5} lombPSD(HR)} \quad (3)$$

For the AB feature, outliers could be eliminated to create a better estimate, however to calculate the heart rate variable (HR) a uniformly sampled and smoothed instantaneous heart rate signal was created using the function “tach” from the WAVE software.

4 Analysis

Each of the individual features was tested to see how well it performed in a recognition task using a linear classifier. Using this classifier each class $k = 1, 2, 3, 4$ was modeled as a gaussian with μ_k equal to the sample mean for that class and σ^2 equal to the pooled variance. The classification was implemented by assigning the feature to the class k for which g_k was maximum[The89] where:

Feature	Rank	Correct	Feature	Rank	Correct
$\mu_{\mathcal{R}}$	1	62.2%	$\sigma_{\mathcal{E}}$	6	53.5 %
$\mu_{\mathcal{G}}$	2	62.0%	ΣS_A	7	53.0 %
ΣS_D	3	58.5%	HR	8	52.6 %
$\mu_{\mathcal{E}}$	4	58.3%	AB	9	52.5 %
S_F	5	57.6%	$\sigma_{\mathcal{R}}$	10	50.2 %
ΣS_M	5	57.6%	$\sigma_{\mathcal{G}}$	11	48.3 %

Table 2: A ranking of each individual feature

Optimal Selected Feature Set	SFFS kNN
AB, HR, ΣS_D , ΣS_M , $\mu_{\mathcal{E}}$, $\mu_{\mathcal{R}}$, $\sigma_{\mathcal{R}}$	88.6 %
AB, HR, ΣS_D , ΣS_M , S_F , $\mu_{\mathcal{G}}$, $\sigma_{\mathcal{G}}$	88.4 %

Table 3: Recognition rates achieved using Jain and Zongker’s FS-SFFS algorithm with a k nearest neighbor classifier. No significant drop in performance occurs when \mathcal{E} and \mathcal{R} are eliminated from the initial pool.

$$g_k(\hat{y}) = \frac{2\mu_k}{\sigma^2}\hat{y} - \frac{\mu_k^2}{\sigma^2} + 2\ln(Pr[w_k]); \quad (4)$$

and the a priori probability of belonging to class k , $Pr[w_k] = \frac{1}{n_k}$ (where n_k is the number of members in class k). For the results in Table 2 leave one out and test cross-validation was used where first μ_k and σ^2 were calculated using all but the feature for one minute, then classifying the excluded feature according to the maximum g_k .

A second analysis was performed using features selected from Jain and Zongker’s sequential forward floating selection (SFFS) algorithm [JZ97]. This algorithm used a k-nearest neighbor classifier and the leave one out and test method and shows that by combining multiple physiological features, the recognition of driver stress can be significantly improved as shown in Table 3. A further feature selection and classification analysis was done eliminating signals which might primarily depend on physical motion, \mathcal{E} and \mathcal{R} , from the initial pool. The result shows no significant decrease in performance indicating both that the stress detected is more likely to be mental and emotional and that high recognition rates can be achieved with few sensors using multiple features.

5 Conclusions

This research shows the application of pattern recognition techniques to the problem of emotional stress detection using features from multiple physiological signals. The results show that by detecting patterns across combinations of features, performance for recognizing stress in drivers improves significantly from at best 62.2% to 88.6%. This performance was shown not to depend mainly on motion artifacts. Perfect performance is not expected due to ambiguities in labeling the stress level, however, the recognition rates from this research suggest that stress information could be used by a computer to control non-critical driving applications, such as as music selection and managing on-board information appliances such as cell phones and navigation aids. In the broader picture, a regular commute offers the opportunity to record daily stress signals for analysis. Records of these stress patterns over time

could provide an indicator of changes in life stress, giving a quantified feedback to the individual about how life choices could be affecting their stress level and providing a new metric with which to make informed choices about their health and behavior.

6 Acknowledgments

The authors would like to acknowledge Kelly Koskelin coding the AB variables, Susan Mosher for data collection, Tom Minka for help with the pattern recognition code and Tanzeem Choudhury for proof-reading. We would also like to thank George Moody and Pr. Roger Mark for the EKG software and Doug Jain and Anil Zongker for the SFFS code. This work was supported by the MIT Media Lab's Digital Life and Things That Think consortia.

References

- [ELF83] Paul Ekman, Robert W. Levenson, and Wallace V. Friesen. Autonomic nervous system activity distinguishes among emotions. *Science*, 221:1208–1210, Sep. 1983.
- [Hel78] M. Helander. Applicability of drivers' electrodermal response to the design of the traffic environment. *Journal of Applied Psychology*, 63(4):481–488, 1978.
- [JZ97] A. Jain and D. Zongker. Feature-selection: Evaluation, application, and small sample performance. *PAMI*, 19(2):153–158, February 1997.
- [Lom76] N. R. Lomb. Least-squares frequency analysis of unequally spaced data. *Astrophysics and Space Science*, 39:447–462, 1976.
- [MAea95] Rollin McCraty, Mike Atkinson, and William Tiller et al. The effects of emotions on short-term power spectrum analysis of heart rate variability. *American Journal of Cardiology*, 76:1089–1093, 1995.
- [Moo93] George B. Moody. Spectral analysis of heart rate without resampling. In *Computers in Cardiology*, pages 715–718, Los Alamitos, CA, 1993. IEEE Computer Society Press.
- [SSea93] J. Paul Spiers, Bernard Silke, and Ultan McDermott et al. Time and frequency domain assessment of heart rate variability: A theoretical and clinical appreciation. *Clinical and Autonomic Research*, 3:145–158, 1993.
- [The89] C. W. Therrien. *Decision Estimation and Classification*. John Wiley and Sons, Inc., New York, 1989.